

CFFT Bridge Columns for Multihazard Resilience

Alicia Echevarria, Ph.D., A.M.ASCE¹; Arash E. Zaghi, Ph.D., P.E., M.ASCE²;
Richard Christenson, Ph.D., M.ASCE³, and Michael Accorsi, Ph.D., M.ASCE⁴

Abstract: Bridges play a significant role in postevent recovery and disaster resiliency of communities. Recent megadisasters, such as the 2011 Great East Japan Earthquake, have prompted the technical community to understand the robustness of infrastructure when subjected to extreme events and the shortcomings of conventional structural systems under multiple hazards. Columns are the most critical load-carrying elements of bridge structures. Enhancing the robustness of bridge columns can improve the resiliency of the bridge itself and the surrounding community by reducing repair costs and downtime after an extreme event. In recent years, the concrete-filled fiber reinforced polymer (FRP) tube (CFFT) system has been widely investigated as a durable and cost-effective alternative design for more robust bridge columns. However, the current AASHTO guide specifications are limited to nonductile, unreinforced CFFT elements. This study summarizes the findings of blast, fire, and seismic experiments performed on CFFT specimens containing minimal longitudinal reinforcement. The residual axial load-carrying capacities of damaged reinforced concrete (RC) and CFFT columns are obtained as a measure of robustness, and estimated restoration times and repair costs are presented for each type of column and each hazard. Subsequently, a set of experimentally validated design equations are developed for the axial and flexural resistance of lightly reinforced CFFT columns in a compatible format with the AASHTO load resistance factor design (LRFD) Guide Specifications for the Design of CFFTs. A formulation for displacement-based seismic design of lightly reinforced CFFT columns is presented, and a provision for the fire protection of this column system is proposed. By presenting a set of experimentally validated design formulations, this study is expected to promote the application of lightly reinforced CFFT columns to enhance the multihazard resilience of bridge infrastructure. DOI: [10.1061/\(ASCE\)ST.1943-541X.0001292](https://doi.org/10.1061/(ASCE)ST.1943-541X.0001292). © 2015 American Society of Civil Engineers.

Author keywords: Multihazard resilience; Concrete-filled fiber-reinforced polymer tube (CFFT); Bridge columns; Special design issues.

Introduction

This paper emphasizes the concept of resiliency by presenting the outcomes of a comprehensive study performed on a novel, multi-hazard-resistant bridge column system used as a robust alternative for conventional reinforced concrete construction. While damage to each individual component of a bridge plays role in the total level of impairment, column failure is understood as the most catastrophic and may result in total loss of bridge functionality. Conversely, other components, such as bearings, abutment backwalls, and shear keys are designed as sacrificial elements that can be repaired or replaced easily in the event of a disaster.

The National Academies (2014) defines resiliency as “the ability to prepare and plan for, absorb, respond, recover from, and more successfully adapt to adverse events.” The application of a column system resistant to multiple artificial and natural extreme events increases resiliency through the following:

¹HNTB Corporation, 2 Gateway Center, Suite 1203, Newark, NJ 07102; formerly, Ph.D. Candidate, Dept. of Civil and Environmental Engineering, Univ. of Connecticut, Storrs, CT 06269 (corresponding author). E-mail: alicia.echevarria@engr.uconn.edu

²Assistant Professor, Dept. of Civil and Environmental Engineering, Univ. of Connecticut, Storrs, CT 06269.

³Associate Professor, Dept. of Civil and Environmental Engineering, Univ. of Connecticut, Storrs, CT 06269.

⁴Senior Associate Dean, School of Engineering, Univ. of Connecticut, Storrs, CT 06269.

Note. This manuscript was submitted on November 1, 2013; approved on January 26, 2015; published online on March 11, 2015. Discussion period open until August 11, 2015; separate discussions must be submitted for individual papers. This paper is part of the *Journal of Structural Engineering*, © ASCE, ISSN 0733-9445/C4015002(16)/\$25.00.

First, a robust system lowers the cost of recovery and downtime by limiting damage to bridge structures. Lee et al. (2013) reports that 67% of bridge failures occurring during earthquakes were due to column failures, 8% were due to foundation failures, and the remaining 25% were due to superstructure elements or connections. Basoz and Kiremidjian (1998) studied bridge damage and repair cost data from the Loma Prieta and Northridge earthquakes. For the Northridge earthquake, bridges with column damage resulted in major global damage, while bridges with no column damage only suffered minor global damage, leading to the inclination that column damage is detrimental to the global functionality of the bridge. Additionally, column damage accounted for an estimated \$8 million in repair costs for bridges suffering major damage. This number is more than half of the total estimated repair or replacement cost when all components are considered.

The Hazus-MH 2.1 Technical Manual (2012) provides restoration functions for highway bridges based on damage states. Not surprisingly, every damage state defined for bridges includes a column damage description. Any bridge experiencing column damage is classified as having extensive damage with a median restoration time of 75 days. Bridges with column collapse are classified as having complete damage with a restoration time of 230 days. Thus, a robust column system that potentially eliminates or reduces column damage may reduce the restoration time to less than one day or by 200%, respectively.

Second, a robust column system improves the postevent functionality of bridge structures, imperative for the recovery of affected regions. Bridges are the most critical elements of surface transportation networks. Uninterrupted function of transportation systems plays a crucial role in disaster response and recovery. After a disaster, communities may suffer for an extended period if a bridge is impassable by first responders, emergency vehicles, or daily traffic.

For instance, the tsunami following the 2011 Tohoku earthquake in Japan washed away the sole bridge to Miyatojima, Miyagi, which isolated the island and 900 residents, and inhibited the crucial supply of food, water, and medical aids ([Kyodo News 2011](#)).

In another study, Pan et al. (unpublished report, 2008) looked at the economic impacts of terrorist attacks or natural disasters on Terminal Island near Los Angeles. The researchers looked at the monetary and employment losses that would be incurred at Terminal Island under three disastrous scenarios. In the first, it was assumed that none of the four major bridges providing access to Terminal Island docks incurred any damage. With no bridge damage, Terminal Island would be shut down for 15 days costing the U.S. economy \$4 billion and 26,000 person-years of employment. In the worst-case scenario, it was assumed that an attack or natural disaster incapacitated the access bridges to the ports for one year. If the bridges were unpassable for one year, the economic losses would be nearly \$45 billion, 11.25 times more than the case with no bridge damage, and the job losses would be almost 280,000 person-years, approximately 11 times more. It was estimated that 35% of these losses impact the immediate Los Angeles and Long Beach, California, area, while the remaining 65% is spread throughout the United States. This study infers the significance of bridge performance in recovery time and damage costs, or resilience.

Bridge columns must retain their axial capacity after an extreme event or series of events to keep the bridge in service or provide first responders and emergency vehicles access to exclusive regions affected by the event(s). The greatest level of resistance for a bridge column occurs if its response to an extreme event yields no loss in axial performance, eliminating the need for postevent repair. If bridge columns remain intact, the resilience will be increased at both structural and societal levels. Studies and models like the aforementioned show that bridge columns not only cause direct economic losses due to bridge repairs but also result in indirect losses due to downtime. Increasing the robustness of bridges by using column systems, such as the system discussed in this paper, can enhance resilience by lessening the burden on a community after an extreme event.

Multihazard resiliency cannot be achieved without application of multihazard resistant components. The sequential devastating events following the Tohoku earthquake including the three major aftershocks of magnitude 7.0 or greater, the tsunami, and the Fukushima nuclear disaster resulted in \$300 billion in damages ([Spacey 2011](#)) and prompted the technical community to improve its understanding of infrastructure resilience to multiple extreme events to develop plans for worst-case scenarios.

Recent publications by the Federal Highway Administration ([FHWA 2011](#)), International Association for Bridge Maintenance and Safety ([IABMAS 2012](#)), and researchers at the University at Buffalo (Lee et al. 2013; Liang and Lee 2013) emphasize the importance of incorporating multihazard resistance into future bridge designs. A combination of multiple hazards acting concurrently or spaced over time may drastically increase the vulnerability of a bridge structure designed for a single extreme event, or one that is independently controlled for more than one extreme scenario. The interrelation of some damaging scenarios that significantly increase the vulnerability of bridge columns including corrosion and earthquake ([Alipour et al. 2011; Choe et al. 2008, 2009; Li et al. 2009; Ghosh and Padgett 2010; Simon et al. 2010; Aquino and Hawkins 2007; Rokneddin et al. 2013](#)), main shock and aftershock ([Franchin and Pinto 2007, 2009; Kumar and Gardoni 2012; Ghosh et al. 2015](#)), and scour and seismic effects ([Alipour et al. 2010, 2013; Prasad and Banerjee 2013](#)) have been previously studied. However, there are still many other possible scenarios affecting

bridge column performance that should be comprehended through extensive research programs. Examples of which are the interaction of independent events, such as fire and earthquake and blast and earthquake, identified by the authors in a separate publication ([Echevarria et al. 2014b](#)).

For such combinations, simply increasing design demands, either force or displacement, on a bridge column has proven to be inadequate due to the complex nature of multievent interactions, which may result in changes in the mode of failure, alterations of the dynamic characteristics of a bridge, and the impairment of material properties or member ductility. Multihazard design encompasses more than an elementary approach of superimposing effects of individual hazards using design load combinations; achieving multihazard resiliency requires looking beyond conventional bridge design and construction methods.

The understanding of the vulnerabilities of reinforced concrete (RC) columns under extreme events laid a foundation for studies focused on improving the design specifications for RC columns in seismic regions ([Kowalsky et al. 1995; Priestly et al. 1996; Priestley 2000; Itani et al. 1997; Mortensen and Saiidi 2002](#)) or threatened by other hazards, such as blast ([Rong and Li 2008; Winget et al. 2005; Williamson and Winget 2005; Williamson et al. 2010](#)).

In parallel, several researchers looked beyond conventional materials and systems. Bridge columns using combined engineered cementitious composites (ECC) and shape memory alloy (SMA) and ultra-high-performance concrete (UHPC) and fiber-reinforced polymers (FRP) have shown improved seismic resistance over RC columns ([Wang and Saiidi 2005; Cruz Noguez and Saiidi 2012; Zohrevand and Mirmiran 2013](#)); concrete-filled steel tubes (CFST) have exhibited resistance to both earthquake and blast ([Fujikura et al. 2007, 2008; Keller et al. 2009; Fujikura and Bruneau 2008, 2011, 2012; Bruneau et al. 2011](#)); and FRP-wrapped concrete columns have exhibited resistance to both seismic and blast events, while providing an improved level of corrosion resistance ([Sadatmanesh et al. 1996; Mirmiran and Shahawy 1997; Berger et al. 2013; Muszynski and Purcell 2003; Sheikh and Yau 2002; Aquino and Hawkins 2007](#)).

In recent years, the concrete-filled fiber-reinforced polymer tube (CFFT) column system has emerged as a high performance alternative to RC bridge columns. Unlike FRP wraps or jackets that serve as retrofit measures for existing columns, the FRP tube of the CFFT system presented herein serves as both formwork and reinforcement for cast-in-place or precast elements for new construction. Static and pseudodynamic tests showed that the structural performance of this column system significantly benefits from the composite action of a FRP tube that acts as the longitudinal and transverse reinforcement, and provides confinement for the concrete core ([Mirmiran and Shahawy 1995, 1996, 1997; Mirmiran et al. 1999, 2000; Fam 2000; Fam and Rizkalla 2002; Fam et al. 2003, 2007](#)). Through more rigorous dynamic studies, the CFFT system has exhibited superb blast, fire, and seismic performance, and its postevent functionality has been proven superior to RC columns ([Zhu et al. 2006; Zaghi et al. 2012; Kavianipour and Saiidi 2012; Echevarria et al. 2014a, b](#)). Zaghi et al. (2012) also acknowledged several construction and durability advantages provided by the CFFT system including reduced construction time and cost by using the FRP as permanent formwork and a self-curing environment for the concrete core and improved corrosion resistance.

Prior to 2012, there were no specifications aiding engineers in the design and implementation of CFFT members. In 2012, AASHTO recently released the 1st Edition LRFD Guide Specifications for Design of CFTTs for Flexural and Axial Members ([2012b](#)), referred to as "Guide Specification" herein. However, the Guide Specification is focused on CFTTs without

any longitudinal or lateral steel reinforcement and provides little guidance for the design of CFFTs subjected to extreme loads that force the column beyond its elastic limit. For columns, the yielding of longitudinal bars is the major source of energy dissipation (Priestly et al. 1996). The absence of steel reinforcement in CFFT columns impairs their ductility and hysteresis damping capacity, thus prohibiting their application as ductile elements under extreme events. Ultimately, this has restricted the bridge construction industry from realizing the benefits of this promising system for multi-hazard resilient design. Beyond its superior structural performance, CFFTs offer radical advantages in bridge construction by eliminating formwork and complex and heavy bar cage fabrication and facilitating accelerated bridge construction (ABC) (Zaghi et al. 2012; Kavianipour and Saiidi 2012).

The presented study is inspired by the fact that the CFFT system makes an excellent candidate for the accelerated construction of cost-effective, highly durable next-generation multihazard-resistant highway bridge columns. To this end, this paper briefly discusses the experimental and analytical results comparing the blast, fire, and seismic robustness of CFFTs containing a minimal amount of reinforcement, with that of conventional RC bridge columns. The measure of robustness is defined herein as a column's ability to retain its axial load-carrying characteristics after exposure to blast, fire, and earthquake hazards. Retention of axial capacity increases the probability that a bridge exposed to an extreme event can resist total collapse, similar to what is illustrated in Fig. 1. If the substructure elements are able to withstand such extreme load conditions, it is likely that the cost and recovery time of the structure itself will be less than if complete failure of the columns occurs.

Subsequently, an interaction equation between axial load and moment capacity (P - M) is proposed for CFFT systems incorporating minimal longitudinal steel reinforcement. The proposed equation is consistent with the Guide Specification format to facilitate the force-based design of CFFT columns. Additionally, axial load-curvature ductility interaction diagrams (P - μ_ϕ) are calculated for displacement-based design typically used in the seismic design of bridges (AASHTO 2011). The presented design guide facilitates the adoption of CFFTs for bridge column construction and brings the community closer to multihazard resistant bridge infrastructure.

The three experimental programs discussed herein demonstrate that CFFTs have the ability to reduce losses in functionality of bridge columns subjected to extreme events. While a community



Fig. 1. Total bridge collapse after column failure (image courtesy of FHWA 2006)

may not be directly aware of the performance of bridge columns after such events, the community feels the repercussions in the form of downtime and repair costs. It should be emphasized that the presented information related to the experimental studies is concise. The focus of this paper is to provide a comparative basis for the multihazard robustness of RC and CFFT systems in terms of axial load-carrying capacity and provide a design methodology for a more resistant column system that can be used for more resilient bridge designs.

Blast Robustness of CFFT Column System

A comprehensive experimental research program studying the blast and fire resistance of RC and CFFT bridge columns was conducted by the University of Connecticut (UConn) (Echevarria et al. 2014a, b). These experiments are briefly discussed herein. The first phase of this project consisted of experimental blast testing at the U.S. Army Engineer Research and Development Center (ERDC) in Vicksburg, Mississippi. Four one-fifth scale columns, two RC and two CFFT, were designed and constructed at UConn and shipped to the ERDC site. Each pair of columns was subjected to two realistic blast threats and later returned to UConn where the residual axial capacities of the damaged columns were determined and used as a comparative measure of robustness for columns subjected to blast.

A steel test frame was designed and fabricated to hold the columns using two steel end caps to replicate pin end conditions. The steel arms were designed to be long enough to ensure that the reflected shock wave, from the solid reaction structure, would not interfere with the columns' responses. Fig. 2 shows the test frame with one of the RC columns in it.

Column Designs

The design of the RC columns was derived from a full-scale prototype and complied with AASHTO Specifications (2012a) for Seismic Zone 1. The RC specimens had a diameter of 203 mm (8 in.) and a height of 1.22 m (48 in.). The longitudinal reinforcement consisted of eight Grade 60, #3- [9.525 mm



Fig. 2. Steel frame used for the blast testing of RC and CFFT columns

(0.375 in.) diameter bars ($\rho_s = 1.75\%$). The transverse reinforcement of the RC columns was provided by 6.35 mm (0.25 in.) diameter smooth wire spirals with a pitch of 63.5 mm (2.5 in.).

At the time of design, AASHTO had not yet released the Guide Specification (2012b). As discussed earlier, a minimal number of longitudinal bars are necessary to compensate for the lack of inelastic energy dissipation of unreinforced CFFT columns. Thus, a reinforcement ratio of approximately 1% was selected to comply with the minimum longitudinal reinforcement according to C5.7.4.2 (AASHTO 2012a) for the CFFT design. The CFFT columns were constructed using a Red Thread II (NOV 2009) FRP pipe with an outer diameter of 219 mm (8.64 in.) and wall thickness of 3.56 mm (0.14 in.). This size of pipe is the closest to the standard 203 mm (8 in.) sonotube that was available to serve as formwork for the RC specimens. The fiber orientation of this particular pipe is aligned at $\pm 55^\circ$ with respect to the longitudinal axis of the pipe, providing both longitudinal and hoop strength to the column. Thus, the longitudinal steel reinforcement of the CFFT columns was reduced to a minimum of six #3- [9.525 mm (0.375 in.) diameter] bars ($\rho_s = 1.12\%$), and no transverse steel reinforcement was included. Fig. 3 shows the reinforcement cages of the RC and CFFT columns. Several strain gauges, free field pressure gauges, and load cells were used to collect the data.

Experimental Blast Tests

Charge weight and standoff distance are the two main parameters that determine the intensity of a specific blast threat. A standoff distance (R), equivalent to the distance from the center of the first lane of traffic to a typical highway bridge column, was used for the testing of all four columns. The charge weight (W) was varied to replicate moderate and severe threats for each column. The value of W for the CFFT-severe threat test was equal to the cubic scale of the maximum amount of TNT that could be carried in a small van or delivery truck (DHS 2009). The value W for the CFFT-moderate test resulted in a peak reflected pressure equal to 80% of the peak

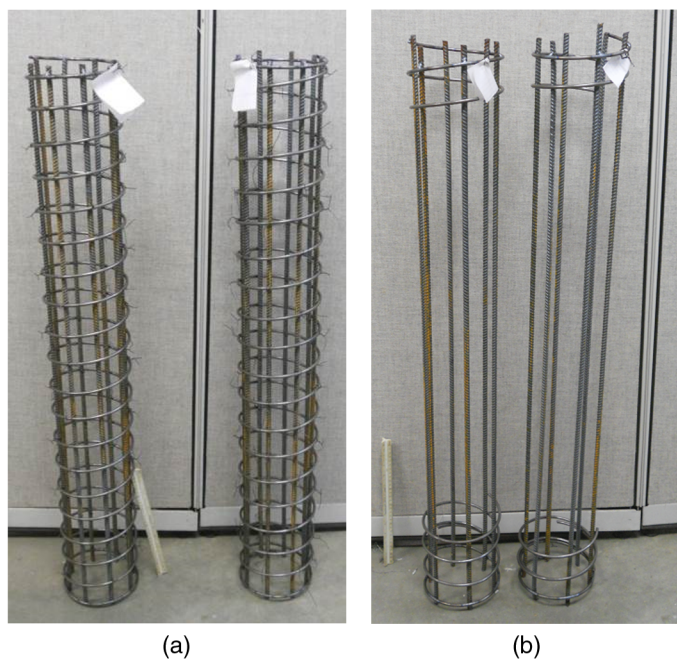


Fig. 3. (a) RC; (b) CFFT rebar cages

Table 1. Final Parameters for Blast Tests

Test number	Column type	Load intensity ratio (LIR)	Charge Wt, W (lbs TNT)	Standoff R (ft)	Scaled standoff, Z (ft/lb ^{1/3})
1	RC	41.1	0.467 W	R	1.23
2	RC	32.9	0.6 W	R	1.14
3	RC	55.6	0.833 W	R	1.02
4	CFFT	41.1	0.733 W	R	1.06
5	CFFT	32.9	W	R	0.958

reflected pressure of the CFFT-severe test. The explicit values of R and W are withheld for security considerations.

Because the RC and CFFT columns have different flexural capacities, a load intensity ratio (LIR), based on moment capacity ratios was used to determine equivalent charge weights for the RC and CFFT moderate and severe tests (Echevarria et al. 2014b). The final relative charge weights and scaled standoff parameter, $W^{1/3}/R$, for all of the tests are presented in Table 1. The CFFT specimens were coated by a fire retardant paint to prevent fire damage to the FRP shell (white coating).

After the moderate and severe threat tests of the RC columns, the only visible damage was charring of the columns' surfaces nearest the charge. To push the limits of the blast study, an additional test was performed on the RC-severe column with an increased charge weight (Test No. 3 in Table 1). After this additional test, observable damage was limited to fine flexural and shear cracks at the center and the bottom of the column, respectively. Although there was no visible damage, peak tensile strains of much larger than the yield strain of steel material were recorded by strain gauges on the longitudinal bars within both sets of columns. The peak strain values and forces recorded by load cells are presented in Table 2. This lack of visible damage after large strains (as large as $16,000 \mu\epsilon$) could be misleading for emergency officials who must decide whether to close a bridge after an explosion. Therefore, it is extremely important to quantify the postblast axial capacity of RC and CFFT columns.

Residual Axial Capacities of Blast-Damaged Columns

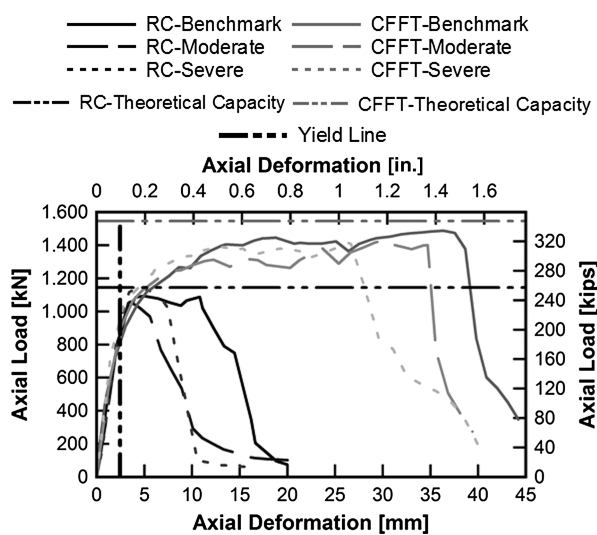
The four blast-damaged columns were returned to UConn's Structures Lab where residual axial capacity testing was conducted using a 1,779 kN (400 kip) Satec load frame controlled by an MTS FlexTest 40 controller. The same end caps used in the blast experiments were installed on the columns before testing using high-strength epoxy grout. Two rigid spherical bearings were used at the ends of specimens to eliminate end fixity moments. A quasi-static multistep axial loading scenario described in Table 3 was used to evaluate the capacity of each column under incremental axial forces. The columns were unloaded to 22.2 kN (5.0 kip) after each step to capture their unloading and reloading characteristics. Four 50-mm (1.97-in.) displacement potentiometers measured relative longitudinal movements and relative rotations of the end

Table 2. Peak Experimental Blast Loads and Strains at Midspan

Test specimen	Peak tension strain ($\mu\epsilon$)	Peak compression strain ($\mu\epsilon$)	Peak total load (kN) (kip)
RC-moderate	3,800	N/A	179 (40.3)
RC-severe	8,500	-2,300	192 (43.1)
RC-severe-2	16,000	-6,700	249 (56.0)
CFFT-moderate	12,200	N/A	224 (50.4)
CFFT-severe	18,100	-7,500	285 (64.0)

Table 3. Axial Loading Scenario

Step	Control type	Increment
1	Force	+222 kN (+50 kip)
2	Force	+222 kN (+50 kip)
3	Force	+222 kN (+50 kip)
4	Force	+222 kN (+50 kip)
5	Force	+222 kN (+50 kip)
6	Displacement	+2.54 mm (+0.1 in.)
7	Displacement	+5.08 mm (+0.2 in.)
8	Displacement	+5.08 mm (+0.2 in.)
9	Displacement	+6.35 mm (+0.25 in.)
10	Displacement	To failure

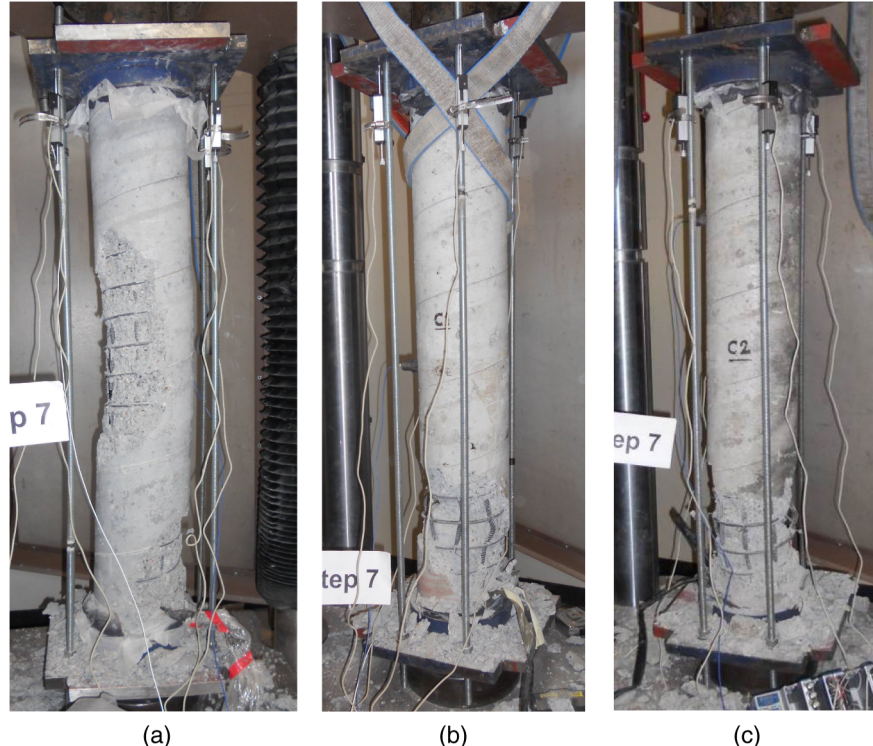
**Fig. 4.** Load-deformation relationships of RC and CFFT blast-damaged columns

caps. The average of these four readings is reported as the axial deformation. In addition to deformations, the load and strain readings on longitudinal bars were also recorded. The test continued until the load significantly dropped.

In addition to the damaged columns, an undamaged benchmark column of each type was tested to determine the uncompromised axial capacity of each column system. The experimental axial load-deformation relationships are presented in Fig. 4. Figs. 5 and 6 show the failed RC and CFFT columns, respectively. The axial capacity of each column at an axial displacement, δ_P , of 10 mm (0.4 in.), axial ductility, and initial axial stiffness were chosen as comparative measures for robustness and are reported in Table 4. This particular value of δ_P corresponds to the point at which the undamaged RC column began to exhibit loss in axial strength. The axial yield displacement is defined as the displacement corresponding to an average axial strain of $2,000 \mu\epsilon$, marked by the yield line in Fig. 4, and the ultimate displacement is defined as the point where load drops to 85% of its maximum.

At $\delta_P = 10$ mm, the axial capacities of the RC columns were compromised by 71.5% and 76.1% after moderate and severe blasts, respectively. Comparatively, the axial capacities of the CFTTs at the same δ_P were not significantly compromised under equivalent blast threats. On average, the axial ductilities of the CFTT columns were 4.25 times the axial ductilities of the RC columns, for each damage state. The RC columns exhibited 19.1% and 31.4% reductions in initial stiffness after moderate and severe blasts, respectively, while the CFTT columns showed no stiffness degradation after equivalent threats. The axial capacity results highlighted the improved robustness of the CFTT system as it was able to retain significantly more capacity than the RC columns under equivalent blast demands.

Fig. 5 shows that the mode of failure of the blast-damaged RC columns was shear failure near the bottom of the column, while the RC benchmark column failed due to concrete crushing near

**Fig. 5.** Failure modes of RC: (a) benchmark; (b) moderate; (c) severe damage columns

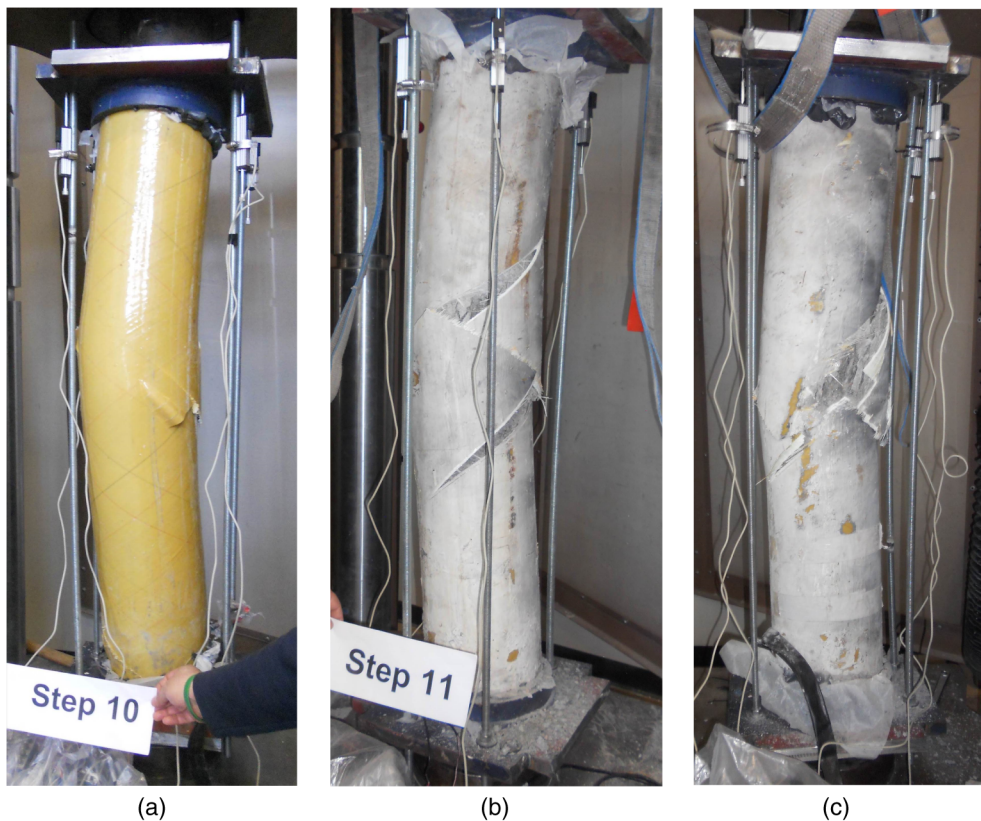


Fig. 6. Failure modes of CFFT: (a) benchmark; (b) moderate; (c) severe damage columns

Table 4. Summary of Axial Test Results of Blast-Damaged Specimens

Axial capacity parameter	RC columns			CFFT columns		
	Benchmark	Moderate	Severe	Benchmark	Moderate	Severe
Capacity at $\delta_P = 10$ mm, kN (kips)	1,075 (242)	306 (68.8)	257 (57.8)	1,276 (287)	1,279 (288)	1,337 (300)
Axial ductility	4.90	2.45	3.12	15.9	14.3	11.4
Axial stiffness, kN/mm (kip/in.)	423 (2,413)	342 (1,953)	290 (1,656)	416 (2,377)	430 (2,460)	502 (2,868)

midspan. All three CFFT columns failed when the FRP shells ruptured at the middle of the columns (Fig. 6). The FRP tube provided significant confinement to the concrete core allowing it to uphold longitudinal strains as large as 2.5%. In addition, it resisted shear crack initiation in the concrete core under blast loading. The experiments demonstrated that although the RC columns showed no outward signs of damage after blast events, the ability of the columns to sustain postyielding axial load was impaired. From a multihazard design perspective, a RC column that is subjected to blast or other types of shock loads, could fail in shear prematurely under a future earthquake, when the stability of a bridge is highly dependent on the flexural yielding of its columns. On the other hand, the performance of the CFFT column system is not impaired by such a sequence of extreme events.

Fire Robustness of CFFT Column System

The second phase of the study was composed of experimental fire testing at Guardian Fire Testing Facility in Buffalo, New York, and subsequent axial load tests on fire-damaged columns. An additional set of four one-fifth scale bridge columns (two RC and two CFFT) having the same design, and constructed at the same time as those

used in the blast experiments, were subjected to two durations of extreme temperatures. Similar to the blast-damaged columns, the columns were returned to UConn where the residual axial load capacities of the fire-damaged columns were found experimentally and used as a comparative measure of fire robustness.

Specimen Preparation and Instrumentation

It is well known that FRP materials do not perform well when directly exposed to fire or extreme temperatures (Gefu et al. 2008; Bisby et al. 2005; Kodur et al. 2007). However, when protected properly, the structural integrity of the CFFT system can be preserved for long periods of exposure to elevated temperatures (Bisby et al. 2005; Kodur et al. 2007). The two CFFT specimens were protected using the Tyfo-CFP fire-protection system (Fyfe 2013). The Tyfo-CFP system is a three-part, low-profile protection system that provides an ASTM 4-h rating with a minimum thickness of 15.9 mm (0.625 in.).

Two Type K thermocouples were installed on each column at the longitudinal bar level and the center of the core to record internal concrete temperatures throughout the fire test. Both thermocouples were placed at the column midspan. Four thermocouples were also used to measure the furnace temperature during testing.

Fire Exposure Experiments

Two separate fire tests following the ASTM E119 testing procedure were conducted. In the first test, titled 1-h, one RC and one CFFT column were exposed to exactly 1 h of elevated furnace temperatures reaching nearly 700°C (1,292°F). For the second test, titled 2-h, the other pair of specimens was exposed to more than 2 h of elevated temperatures extending to 800°C (1,472°F). The durations and temperatures of these tests are comparable to those reported as part of NCHRP 12-85 (Wright et al. 2013). The furnace temperature time histories measured by the four thermocouples and the average temperature of the two tests can be seen in Figs. 7(a and b), respectively. The RC and CFFT concrete temperatures recorded during the 1 and 2-h tests are provided in Figs. 8(a and b), respectively. During the 1-h test, the maximum temperatures at the reinforcement level and core reached to 283°C (541°F) and 183°C (361°F), and 91°C (196°F) and 82°C (180°F) for the RC and CFFT columns, respectively. The same values were measured as 491°C (916°F) and 431°C (808°F), and 160°C (320°F) and 143°C (289°F) in the 2-h experiment.

From Chang et al. (2006), concrete compressive strength, f'_c , and compressive elastic modulus, E_c , are reduced to 90% and 80% of those of intact material, respectively, when concrete temperatures reach 200°C (392°F). At 400°C (752°F), f'_c and E_c drop

to 65 and 40% of original values, respectively. Two reference lines at 200°C (392°F) and 400°C (752°F) are shown in Fig. 8 implying that some level of deterioration of concrete material was expected in the RC specimens. The protection applied to the CFFT columns effectively kept the temperatures of the concrete significantly lower than that of the RC columns, preserving both the strength and elastic stiffness of concrete material.

The fire-damaged RC columns had no visible sign of damage and could not be visually distinguished from the intact column. Although engineers would likely conduct more than visual observations after a major fire event, the lack of visual damage could be misleading for onsite postevent evaluations. If strength loss is suspected, Wright et al. (2013) recommend destructive testing to accurately quantify the loss.

Residual Axial Capacities of Fire-Damaged Columns

The same axial load test method previously described for the blast-damaged columns was used to determine residual axial capacities, ductilities, and stiffnesses of the fire-exposed columns. Fig. 9 shows the axial load-deformation relationships. Figs. 10 and 11 show the status of each column after failure under axial load. The RC 2-h specimen lost its cover along most of its length due to the extensive deterioration of the concrete material. The same

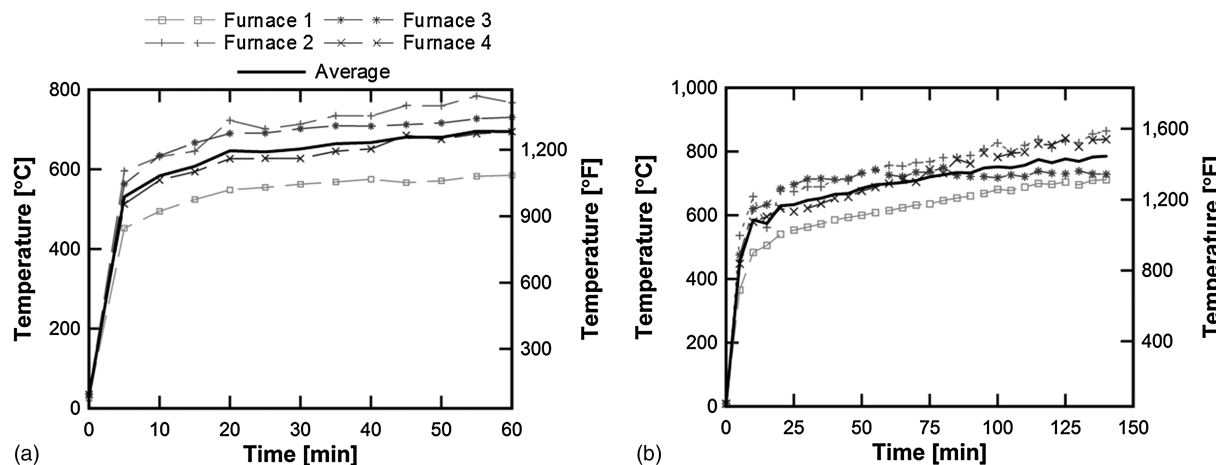


Fig. 7. Furnace temperatures for (a) 1-h fire test; (b) 2-h fire test

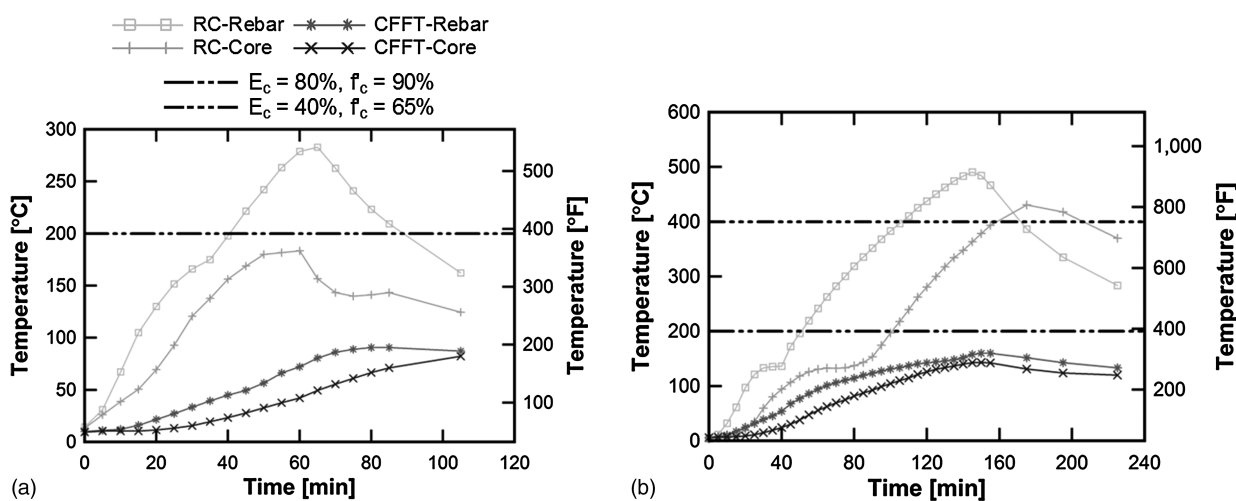


Fig. 8. Concrete temperatures for (a) 1-h fire test; (b) 2-h fire test

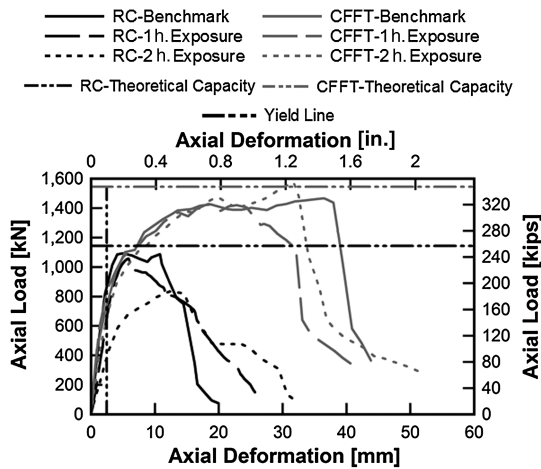


Fig. 9. Load-deformation relationships of RC and CFFT fire damaged columns

measures of robustness used for the blast-damaged columns (axial capacity at $\delta_p = 10$ mm, axial ductility, and initial axial stiffness) were used to evaluate the fire-damaged columns. The test data for each fire-damaged column and the respective benchmark columns are shown in Table 5. While the fire-damaged RC columns exhibited losses of 15.4% and 26.6% in axial capacity and 41.7% and 66.5% in initial stiffness after 1 and 2-h exposure, respectively, the protected CFFT specimens showed no meaningful loss in axial strength and just a 25% loss in stiffness after 2-h exposure, further proving the robustness of the CFFT system. Once again, from a multihazard design point of view, a fire-damaged RC column

may fail in a brittle fashion and under much smaller demands when subjected to a future extreme event.

Seismic Robustness of CFFT Column System

As part of a research project conducted at the University of Nevada, Reno (UNR) (Zaghi et al. 2012), a scaled two-column bridge pier integrating one RC column and one CFFT column was subjected to simulated ground motions using a shaking table. The seismic performance of the CFFT columns had previously been studied through pseudodynamic testing (Mirmiran and Shahawy 1995, 1996; Mirmiran et al. 1999, 2000; Shao 2003; Shao and Mirmiran 2004, 2005; Zhu et al. 2004, 2006), but the shaking table experiment at UNR was the first to compare the performance of CFFT and RC columns subjected to identical dynamic displacements. A brief overview of this experiment is presented herein. Further details are presented by Zaghi et al. (2012).

Specimen Design and Shaking Table Test Results

The RC and CFFT columns were designed to have comparable lateral load capacity at a 5% drift ratio. Because no axial test data was planned as part of the experiment, the largest diameter column that could be pushed to failure without exceeding the shaking table capacity was selected. The CFFT column incorporated a 370-mm (14.5-in.) outside diameter Red Thread II (NOV 2009) FRP pipe with a wall thickness of 7 mm (0.27 in.). The CFFT column contained eight, #4- [12.7 mm- (0.5 in.) diameter] longitudinal reinforcing bars ($\rho_s = 1.04\%$). The conventional RC column was 356 mm (14 in.) in diameter and consisted of 20 #4- [12.7 mm- (0.5 in.) diameter] longitudinal bars ($\rho_s = 2.6\%$).

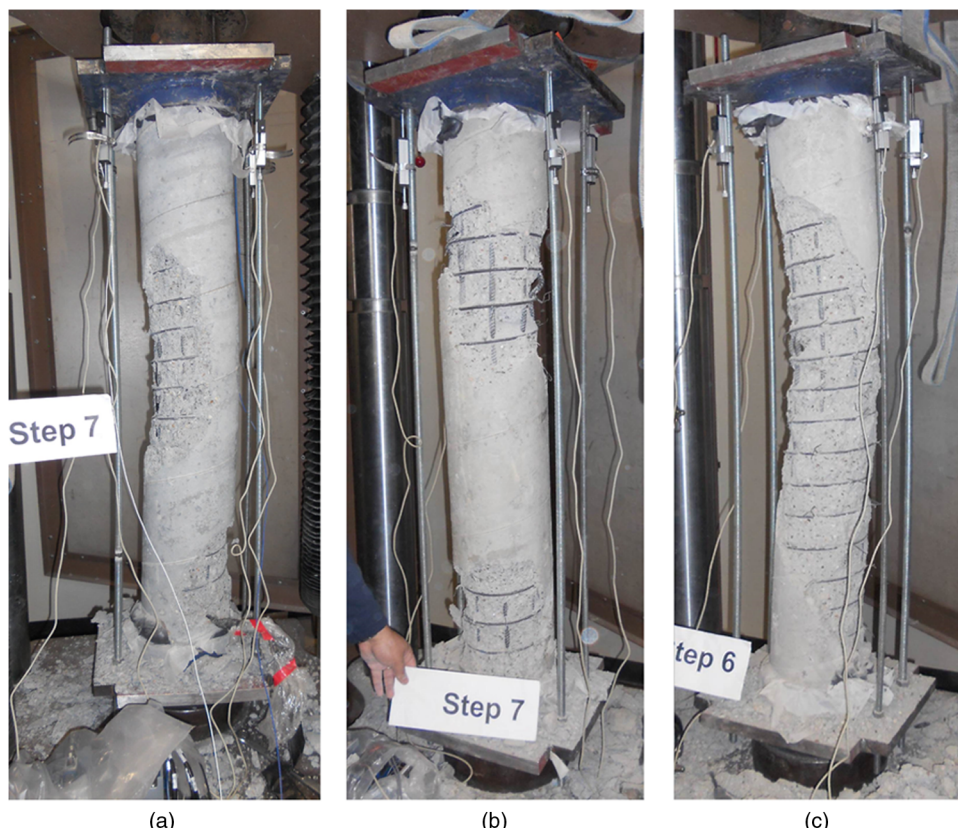


Fig. 10. Failure modes of RC: (a) benchmark; (b) 1-h; (c) 2-h exposure columns

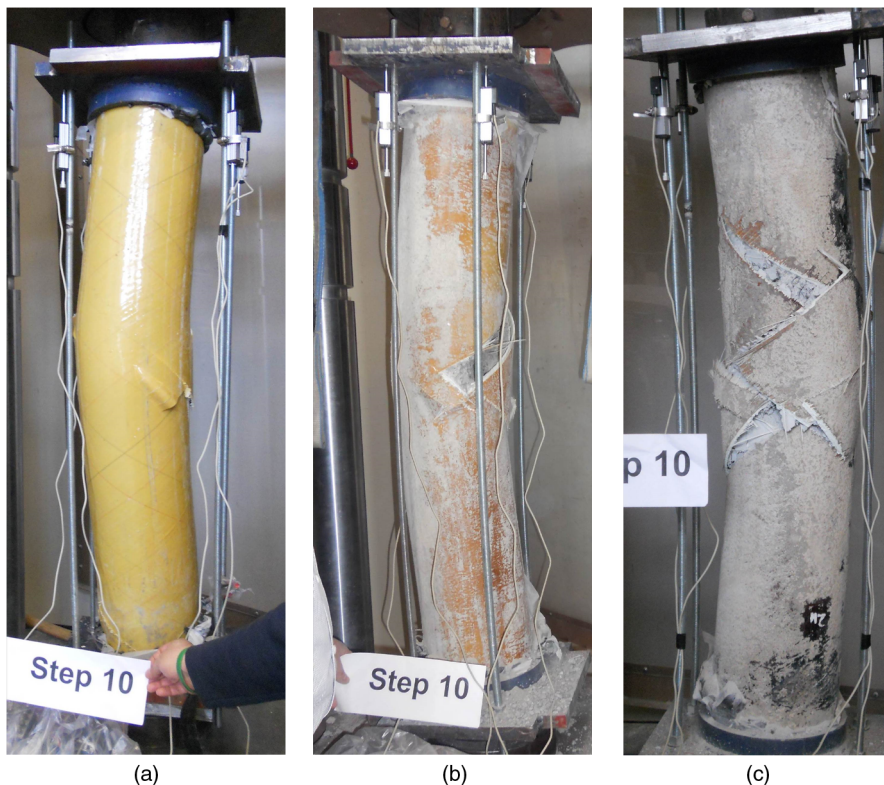


Fig. 11. Failure modes of CFFT: (a) benchmark; (b) 1-h; (c) 2-h columns

Table 5. Summary of Test Capacity Results of Fire-Damaged Specimens

Axial capacity parameter	RC columns			CFFT columns		
	Benchmark	1-h exposure	2-h exposure	Benchmark	1-h exposure	2-h exposure
Capacity at $\delta_p = 10$ mm, kN (kip)	1,075 (242)	909 (204)	789 (177)	1,276 (287)	1,242 (279)	1,210 (272)
Axial ductility	4.90	4.27	6.44	15.9	11.9	13.5
Axial stiffness, kN/mm (kip/in.)	423 (2,413)	246 (1,406)	142 (808)	416 (2,377)	443 (2,529)	310 (1,772)



Fig. 12. Construction of RC and CFFT two column bent

A two-way hinge connection was used at the tops of the columns. The embedment length of the CFFT column into the footing was 1.5 times the column diameter. Fig. 12 shows the bent before the footing was cast.

The two-column pier model was subjected to seven uniaxial shaking table runs of 0.1, 0.4, 0.7, 1.0, 1.3, 1.6, and 1.9 times the ground acceleration recorded at the Sylmar Converter Station during the 1994 Northridge earthquake. While the CFFT column exhibited no signs of damage until the seventh shake table run (PGA = 1.73 g), spalling of the cover of the RC column started during Run 4 (PGA = 0.91 g). During the last run, the maximum displacement ductility of the CFFT and RC columns were measured as 12.2 and 10.5, respectively. The CFFT column exhibited a plastic hinge length double that of the RC column, which contributed to 60% more energy dissipation with respect to the steel ratio of each column. The ductility and hysteresis energy dissipation capacity of the CFFT system including a small percentage of reinforcement led to the conclusion that the CFFT system is a valid alternative for the seismic design of RC bridge columns.

Residual Axial Capacity of Earthquake-Damaged Columns

Unlike the blast-damaged and fire-damaged columns, the residual axial capacities of seismic-damaged columns were evaluated using analytical models of CFFT and RC columns. OpenSees software ([PEER 2012](#)) was used to simulate the shaking table response of the UNR two-column bent based on the nonlinear fiber section modeling technique used by Zaghi et al. ([2012](#)). This modeling

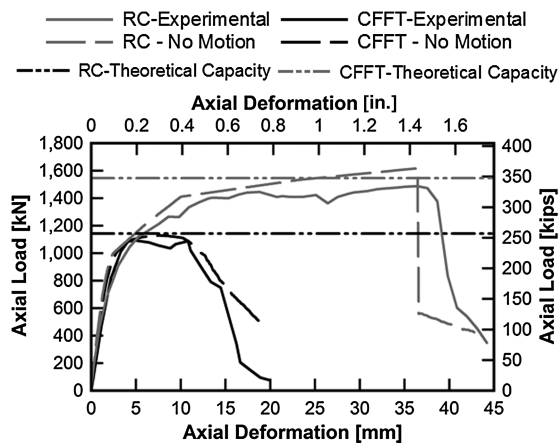


Fig. 13. Comparison of analytical model and experimental columns with no damage

method was further validated using the results from the axial capacity experiments conducted at UConn on the benchmark CFFT and RC columns. Fig. 13 shows the comparison of analytical results with those obtained from axial experiments.

The validated modeling method was used to investigate the adverse effect of seismic damage on the axial load capacity of RC and CFFT systems. To this end, two columns with designs similar to those of the one-fifth scale blast and fire test columns were modeled in OpenSees. The models were subjected to two intensities of biaxial ground motion, and subsequently pushed axially to obtain the residual axial capacities of the damaged columns. Each column was

modeled as a cantilever with an axial dead load equivalent to 10% of the column's full axial capacity, which is typical of axial load value in bridge columns. A lateral mass corresponding to the dead load was assigned to the end of the columns.

The horizontal ground accelerations recorded from the Sylmar Olive View Medical Center during the 1994 Northridge earthquake were scaled separately for each column to result in lateral drifts of 4 and 7% to impose moderate and severe levels of seismic damage to the columns. After each nonlinear time-history analysis, the residual axial capacities of the columns were determined through a displacement-controlled axial pushover analysis. The MinMax material of OpenSees was used to eliminate the contribution of FRP fibers that exceed 7 and 3% strain in axial tension and compression, respectively. After experiencing 4 and 7% peak lateral drifts, the axial load-displacement relationships for the seismic-damaged RC and CFFT columns were compared with the results of the columns prior to any imposed ground motion as shown in Fig. 14.

The axial capacity of each column at $\delta_p = 10$ mm, axial ductility, and initial axial stiffness are reported in Table 6. At this axial displacement, the capacity of the RC column was compromised by 52.0 and 66.2% after experiencing 4 and 7% peak lateral drifts, respectively. Comparatively, the axial capacity of the CFFT at the same axial strain was compromised by only 0.35 and 3.69% under the same drift levels. Additionally, the average axial ductility of the CFFT column was 3.21 times that of the RC column for each damage level. Aside from strength and ductility, the RC and CFFT columns exhibited comparable reductions in axial stiffness after each level of drift.

AASHTO Guide Specifications for CFFT Design

AASHTO has recently released the 1st edition of LRFD Guide Specifications for Design of CFFTs as Flexural and Axial Members (AASHTO 2012b). The Guide Specification serves as a supplement to the AASHTO LRFD Bridge Design Specifications (AASHTO 2012a) for the analysis and design of CFFTs as structural components in bridges. The Guide Specification includes equations for the capacity of CFFT members subjected to flexure, axial compression, and combined flexure and axial compression. Although the Guide Specification enables the use of CFFT components in bridge design, it lacks pivotal aspects that would allow CFFTs to be used as columns for a multihazard resilient bridge design.

The Guide Specification limits the multihazard design of the CFFT system in two ways. First, the Guide Specification limits the applicability of the CFFT system for extreme events. Section 1.3 explicitly states that CFFTs shall not be used as ductile earthquake-resisting elements (AASHTO 2012b). Section 2.7.4 of the Guide Specification states that a structure consisting of CFFT members shall be proportioned to resist collapse due to extreme events, specified in Table 3.4.1-1 of AASHTO-LRFD (AASHTO 2012a). While earthquake loads and blast loads are included in the table, no guidance is provided for the design of CFFT members that

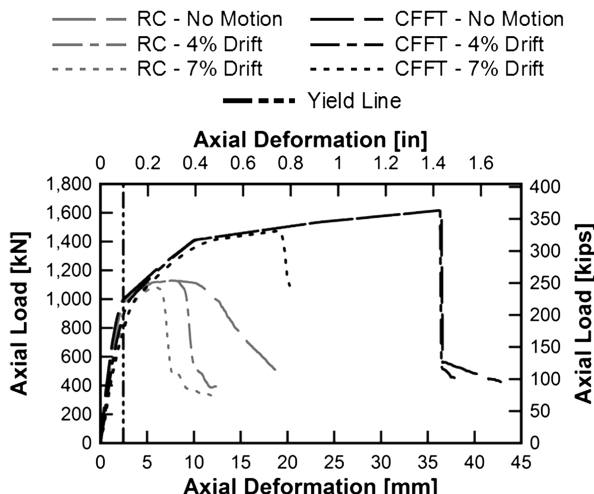


Fig. 14. Load-deformation relationships of earthquake-damaged RC and CFFT columns

Table 6. Residual Axial Capacity Results of RC and CFFT Columns Subjected to Seismic Load

Axial capacity parameter	RC columns			CFFT columns		
	No motion	4% drift	7% drift	No motion	4% drift	7% drift
Capacity at $\delta_p = 10$ mm, kN (kip)	1,114 (250)	535 (120)	377 (84.8)	1,410 (317)	1,405 (316)	1,358 (305)
Axial ductility	5.27	3.80	2.83	14.95	14.90	8.12
Axial stiffness, (kN/mm) (kip/in.)	625 (3,566)	562 (3,207)	492 (2,812)	674 (3,846)	478 (2,729)	440 (2,512)

may be subjected to such loading, nor are there any provisions for fire protection of the system.

The second limitation of the Guide Specification is that its axial compression and flexural resistance equations do not account for longitudinal steel reinforcement within CFFT members. Experiments conducted by Mohamed and Masmoudi (2010) include CFFT specimens both with and without steel reinforcement. Longitudinal steel is not necessary to significantly increase the static axial resistance of CFTTs. However, the blast and seismic studies previously summarized have indicated that modest amounts of longitudinal steel reinforcement can positively impact the ductility and energy dissipation performance of CFTTs subjected to extreme events. In fact, with a steel reinforcement ratio of around 1.0% and fire protection, CFTT columns outperform and exhibit superior resistance to blast, fire, and earthquake compared to conventional RC columns (Zaghi et al. 2012; Echevarria et al. 2014a, b). Including a small amount of longitudinal steel can provide the CFTT system with the strength and ductility needed to prevent a total collapse, and even maintain the serviceability of a bridge structure after extreme events.

Proposed Design Method for a Ductile CFFT System

A new set of axial and flexural resistance equations consistent with the Guide Specification and Seismic Specifications (AASHTO 2011) format are developed as part of this study. The equations include the added resistance of longitudinal steel reinforcement for multihazard resistant CFFT design. The new resistance equations along with a combined axial-flexural (P - M) interaction equation are presented for force-based CFFT design. Additionally, a set of curvature ductility curves with respect to the axial load of a column are presented for the displacement-based design method used for the seismic design of bridge components (AASHTO 2011; Caltrans 2006).

While the proposed resistance equations and ductility relationships provide a means to determine the strength and displacement capacity of CFFT columns, they do little to preserve the resistance of the system to extreme temperatures. It is recommended to include a provision that requires CFTTs to be coated with a fire-protection system that has a minimum 4-h rating to achieve fire resistance.

Axial and Flexural Resistance of CFFT Columns with Internal Reinforcement

Rigorous moment-curvature analyses of a generic CFFT cross section, shown in Fig. 15, were performed using XTract software (Imbsen 2007). The steel reinforcement ratio, ρ_s , was varied between 0.002 and 0.016 to develop a set of capacity equations. The FRP tube used for the development of the capacity equations is assumed to have a fiber orientation of $\pm 55^\circ$ with respect to the longitudinal axis of the column. This fiber alignment proved to be structurally efficient in resisting blast and seismic loads, and sustaining postyielding axial forces. In this generalized section the concrete core diameter to shell thickness, D/t , was assumed to have a constant value of 60 based on an average of the Red Thread II FRP tubes (NOV Fiberglass Systems 2009).

The FRP tube was modeled using the hysteretic FRP material model presented by Zaghi et al. (2012). The experimental results of the axial compression tests performed by Echevarria et al. (2014a, b) and shaking table tests by Zaghi et al. (2012) were used to determine the compression and tension rupture strains of the FRP material. A rupture strain of $30,000 \mu\epsilon$ was measured on the FRP tube during the axial testing of the undamaged column.

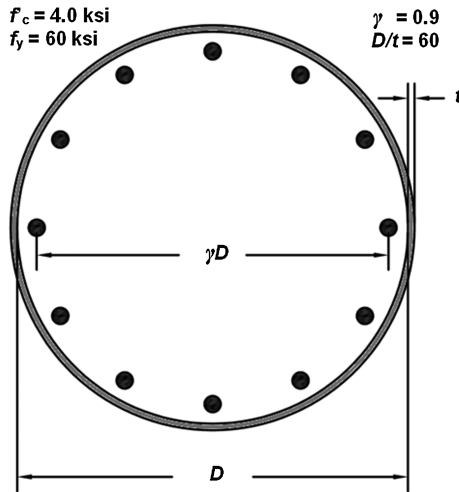


Fig. 15. Generic cross section for moment-curvature analyses of CFFT columns

In the experiments performed by Zaghi et al. (2012), tension rupture of the FRP tube was observed at a strain of $70,000 \mu\epsilon$, while no compression failure was reported during the shaking table experiments. Thus, $30,000 \mu\epsilon$ and $70,000 \mu\epsilon$ are the assumed compression and tension strain limits of the FRP tube, respectively. The steel reinforcement is assumed to be ASTM A615 Grade 60 with an expected yield strain of $2,300 \mu\epsilon$ and ultimate tensile strain of $90,000 \mu\epsilon$ (AASHTO 2011). The confined concrete core was modeled following the backbone curve presented in Fig. 16. On this curve, ε_{co} and f'_{co} correspond to the break point suggested by Lam and Teng (2003) where f_{co} is the unconfined compressive strength of the concrete and ε_{co} is calculated using Eq. (1)

$$\varepsilon_{co} = \frac{2f_{co}}{E_c - E_2} \quad (1)$$

where E_c = elastic modulus of unconfined concrete; and E_2 = slope of the linear second branch calculated as

$$E_2 = \frac{f_{cu} - f_{co}}{\varepsilon_{cu}} \quad (2)$$

The values of ε_{cu} and f_{cu} are determined following AASHTO specifications for FRP-confined concrete compressive strain and strength, respectively (AASHTO 2012b). After the concrete strain

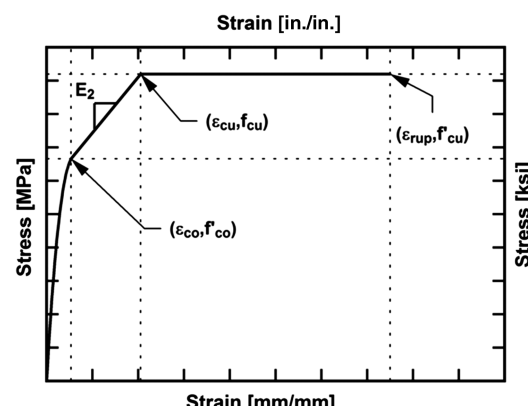


Fig. 16. Stress-strain relationship of FRP-confined concrete

surpasses ε_{cu} , its stress remains constant at f_{cu} until reaching the rupture strain, ε_{rup} . The experiments performed in this study showed no loss in strength until the rupture of the FRP tubes. Thus, the value of ε_{rup} is assumed equal to the compressive rupture strain of the FRP tube.

The results of the moment-curvature analyses were compiled to develop equations for the nominal axial and flexural capacities, as well as a combined P - M interaction equation for CFFT columns with longitudinal steel reinforcement. The axial load index (ALI) of a column is defined as the compressive load divided by the product of the gross cross sectional area and the unconfined concrete compressive strength. The typical range of ALI for bridge columns is 5–25% with the recommended value being 10% for seismic regions (Correal et al. 2004). For this reason, the proposed equations have been optimized only for ALI's less than or equal to 25%. The results of 110 moment-curvature analyses were summarized to the following equations using regression analysis.

- Nominal axial capacity under pure compression

$$P_n = (1.5 + 18\rho_s)f'_c A_g \quad (3)$$

- Nominal moment capacity under pure flexure

$$M_n = (0.135 + 7\rho_s)f^*A_g D \quad (4)$$

- For CFFTs under combined loading, the applied axial and flexural loads P and M , respectively, must satisfy

$$\frac{M}{M_n} = 1 + \alpha \left(\frac{P}{P_n} \right) + \beta \left(\frac{P}{P_n} \right)^2 \quad (5)$$

$$\alpha = 3.75 - 140\rho_s \quad (6)$$

$$\beta = -8.25 + 200\rho_s \quad (7)$$

where P_n = nominal axial compressive resistance of the cross section with no flexural load; M_n = nominal flexural resistance with no axial load; A_g = gross area of the CFFT cross section; f'_c = specified unconfined concrete compressive strength; f^* = 4.0 ksi; D = diameter of the concrete core; and ρ_s = longitudinal steel reinforcement ratio (the ratio of the area of steel reinforcement to the gross cross section area). In Eq. (4), f^* is used to normalize the flexural capacity. In the moment-curvature analyses, it is assumed to have the same value as f'_c . However, for cases where f'_c is larger or smaller than 4.0 ksi, the value of f^* shall remain set to 4.0 ksi, as the flexural capacity of CFFTs is not significantly affected by the compressive strength of the concrete, and scaling the flexural capacity directly by f'_c results in unrealistic values. Conversely, the axial capacity of CFFTs is

heavily dependent on the compressive strength concrete. Thus, f'_c is directly used in Eq. (3) to normalize the axial load capacity.

Table 7 compares the axial and flexural capacities of the generic CFFT column (Fig. 15) with varying ρ_s and ALI values obtained from refined moment-curvature analyses with the axial and flexural capacities found through utilization of the presented resistance equations. The largest margin of error is 1.71% for all values of axial and moment capacity when compared to moment-curvature analyses, which demonstrates that the proposed equations are accurate for ALI's less than 25%.

To further validate these equations, the experimental axial capacity of the benchmark CFFT column from the axial experiments conducted at UConn was compared to the axial resistance calculated using Eq. (3). It should be noted that Eq. (3) is developed based on the capacity of the cross section and is valid for short nonslender columns. Per AASHTO LRFD (2012a), the axial capacity of compression members is based on the capacity of the cross section for members not braced against unbraced against sidesway with slenderness ratio, KL/r , less than 22 and members braced against sidesway with $KL/r < 34 - 12(M_1/M_2)$, where M_1 and M_2 are the smaller and larger end moments, respectively. Because the experimental specimens were braced against sidesway during the axial capacity tests and had $KL/r = 22.2$, the axial capacity of the columns can be accurately determined based on capacity of the cross section. The experimental axial capacity of the column was obtained as 1,487.5 kN (334.4 kip), and the nominal axial capacity from Eq. (3) is 1,478.7 kN (332.4 kip). This confirms that the proposed equation is reliable for determining the axial capacity of a nonslender CFFT column.

Next, the moment capacity of the CFFT column tested on a shaking table at UNR was used to verify the interaction equation [Eq. (5)]. The maximum base shear force and lateral displacement of the CFFT column recorded during the last run of the shaking table tests were 197.9 kN (44.5 kip) and 137.2 mm (5.4 in.), respectively (Zaghi et al. 2012). The axial load on the CFFT column at its maximum lateral displacement was 311.4 kN (70 kip), resulting in ALI = 6.11%. By multiplying the maximum base shear by the length of the column, and assuming that the axial load acts at the center of the bearing area at top of the column, the ultimate moment capacity, including the P -Delta effects, was 324.6 kN-m (2,874 kip-in.). The moment capacity determined by Eq. (5) is modified to account for the actual yield strength of steel reinforcement and the actual D/t ratio of the CFFT column in the shaking table tests. To do so, the predicted moment is scaled by the ratio of actual steel strength (75 ksi) to the generic steel strength of 60 ksi, and by the ratio of the generic D/t ratio of 60 to the actual D/t ratio of 52.15. The scaled moment capacity is computed as 326.8 kN-m (2,892 kip-in.), confirming the accuracy of Eq. (5).

Table 7. Comparison of Axial and Flexural Capacities Obtained from Cross Section Analysis and Proposed Design Equations

Normalized axial or flexural capacity	Steel ratio (ρ_s)									
	0.002		0.006		0.008		0.01		0.016	
	Section analysis	Design equation	Section analysis	Design equation	Section analysis	Design equation	Section analysis	Design equation	Section analysis	Design equation
P	1.521	1.536	1.589	1.608	1.629	1.644	1.663	1.680	1.771	1.788
$\bar{M}_{ALI=0\%}$	0.150	0.149	0.176	0.177	0.191	0.191	0.205	0.205	0.245	0.247
$\bar{M}_{ALI=5\%}$	0.164	0.165	0.189	0.192	0.205	0.205	0.218	0.218	0.257	0.256
$\bar{M}_{ALI=10\%}$	0.178	0.178	0.202	0.204	0.217	0.217	0.229	0.229	0.263	0.264
$\bar{M}_{ALI=15\%}$	0.190	0.188	0.212	0.214	0.224	0.226	0.236	0.238	0.269	0.270
$\bar{M}_{ALI=20\%}$	0.197	0.196	0.218	0.222	0.230	0.233	0.241	0.244	0.273	0.273

Note: $\bar{M} = M_n/(f'_c A_g D)$; $P = P_n/(f'_c A_g)$.

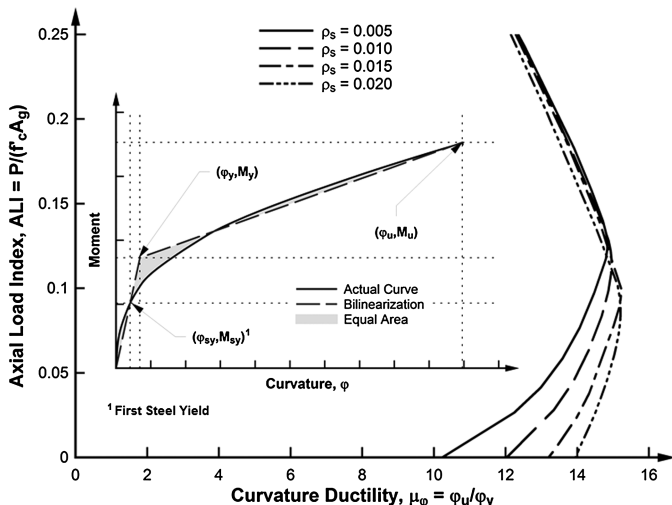


Fig. 17. Curvature ductility of CFFT columns and bilinearization method (inset)

Displacement Capacity of CFFT Columns with Internal Reinforcement

To enable displacement-based seismic design of CFFT columns (AASHTO 2011), the moment-curvature relationships were used to develop curvature ductility-axial load relationships. A sample set of these curves are presented in Fig. 17. For columns with $ALI < 10\%$, the curvature ductility is significantly increased with increasing amounts of steel reinforcement. For columns with $ALI > 10\%$, steel reinforcement has a lesser role in curvature ductility. The curvature ductility, μ_ϕ , of a column can be used to determine the displacement ductility of the column using Equation C4.9-6 of the AASHTO Seismic Specifications (2011). Although the displacement-based design methodology described by AASHTO assumes an elastic-perfectly plastic moment-curvature relationship for reinforced concrete members, an elastic-plastic bilinearization with postyield hardening is more appropriate for CFFT columns due to the large postyielding slope of the moment-curvature relationships (Fig. 17). In addition, a plastic hinge length of $1.45D$ for CFFT columns is proposed by Zaghi et al. (2012).

The presented ductility curves were validated using the experimental results of Zaghi et al. (2012). From the presented curves, a CFFT column with $\rho_s = 0.010$ and $ALI = 6.11\%$ has a curvature ductility, μ_ϕ , of 14.27. This value leads to a displacement ductility, μ_D , of 12.22 using Eq. (C4.9-6) (AASHTO 2011). The displacement ductility reported by Zaghi et al. during the shaking table experiments was 12.2, providing a validation for the proposed curvature ductility curves.

Discussion

A multihazard-resistant bridge column system has been presented as a robust alternative to conventional reinforced concrete construction. The use of multihazard-resistant systems like the one presented can improve resiliency by lessening the cost of recovery and downtime by limiting damage to and maintaining the post-event functionality of bridge structures, imperative for the recovery of affected regions. Table 8 compares estimated restoration times and repair costs for a bridge with conventional RC columns and one with CFFT columns subjected to each of the three hazards presented. The cost and time of postevent evaluation of columns are assumed to be 2% of the bridge construction cost and less than one day, respectively.

Conclusions

The following observations and conclusions are made from this study:

- Improved resiliency may be achieved through using an alternative multihazard-resistant bridge column system that maintains functionality of bridges after an extreme event. The time and cost recovery may be significantly reduced if damage to bridge columns is diminished or reduced. Using the CFFT column system increases resiliency through preserving the axial capacity.
- Recent blast, fire, and shaking table experiments have revealed that CFFT column systems that contain small amounts of longitudinal reinforcement and are properly protected against fire provide a design alternative to conventional RC bridge columns for multihazard resilient bridge infrastructure.
- Because the concrete material is highly confined by FRP tube, the intact CFFT column system has significantly larger axial ductility compared to the conventional RC column system.
- Blast, fire, and seismic damages reduced the axial capacity, axial stiffness, and axial ductility of the RC system. CFFT columns resisted the extreme events while maintaining their performance under axial loads.
- The moderate and severe blasts caused premature shear failure and reduced the axial capacity of RC columns by 71.5 and 76.1%, respectively. The axial stiffness of RC columns was also reduced by 19.1 and 31.4% after moderate and severe blasts, respectively. Neither the axial capacity nor the axial stiffness of the CFFT system was impaired by moderate or severe blast. Additionally, the blast-damaged CFFTs had an average axial ductility 9.49 times that of the blast-damaged RC columns.
- The RC columns exhibited losses of 15.4 and 26.6% in axial capacity and 41.8 and 66.4% in initial axial stiffness under 1 and 2-h exposure to extreme temperature, respectively. Protected CFFTs exhibited no meaningful loss in axial capacity after the same durations of exposure, and just a 25.5% loss

Table 8. Estimated Highway Bridge Restoration Time and Cost Based on Column Performance

Hazard type	Intensity	RC columns			CFFT columns		
		Column damage	Restoration time ^a (days)	Repair cost ^b (%)	Column damage	Restoration time ^a	Repair cost ^b (%)
Blast	$Z > 1.0 \text{ ft/lb}^{1/3}$	Moderate/extensive	2–75	5–25	Slight/minor	<1 day	2
	$Z < 1.0 \text{ ft/lb}^{1/3}$	Extensive/complete	75–225	25–100	Moderate	2 days	10
Fire	1-h duration	Moderate	2	10	Slight/minor	<1 day	2
	2-h duration	Complete	225	100	Slight/minor	<1 day	2
Earthquake	$PGA < 1.0 \text{ g}$	Moderate/extensive	2–75	5–25	Slight/minor	<1 day	2
	$PGA > 1.0 \text{ g}$	Extensive/complete	75–225	25–100	Moderate	2 days	10

^aEstimates are based on Hazus (2012) highway bridge information.

^bAs a percentage of bridge replacement cost.

in initial axial stiffness after 2-h exposure. The significant loss of axial strength and stiffness observed in the fire-damaged RC columns resulted in larger values of axial ductility when compared to the undamaged column.

- The RC column design exhibited losses of 52.0%, 10.1%, and 27.9% in axial strength, stiffness, and ductility, respectively, after experiencing 4% lateral drift. The CFFT system, under the same drift level, had losses of 0.35%, 29.0%, and 0.33% for the same resistance measures. After 7% drift, the RC column lost 66.2%, 21.3%, and 46.3% of its axial strength, stiffness, and ductility, respectively, while the CFFT column lost 3.69%, 34.7%, and 45.7% for the same resistance measures.
- The proposed formulation for lightly reinforced CFFTs was able to predict the axial and flexural capacity of CFFT columns with less than 1% error when compared to experimental values.
- The presented $P-\mu_\phi$ curves used in conjunction with Eq. (C4.9-6) (AASHTO 2011) were able to accurately predict the displacement ductility of a CFFT column tested on a shaking table at UNR.

The work presented in this study is focused on comparing the postevent performance of RC and CFFT columns subjected to independent blast, fire, and seismic hazards. Although it has been shown that CFFT columns perform favorably during and after each of these events, more research is needed to study how bridge columns perform throughout their lifespan when subjected to multiple hazards acting both simultaneously and subsequently. Additional experiments on both RC and CFFT systems would also result in supplemental data that could be valuable for future reliability-based design methods for multihazard-resistant bridge columns.

Acknowledgments

This material is based upon work supported by the U.S. Department of Homeland Security under the DHS HS-STEM Career Development Grant Award Number 2008-ST-061-TS002. The views and conclusions contained in this document are those of the authors and should not be interpreted as necessarily representing the official policies, either expressed or implied, of the U.S. Department of Homeland Security. Vince Chiarito, Stanley Woodson, Jared Minor, Larry Garrett, Clifford Grey, Arnette Nash, and many others from USACE-ERDC are thanked for the assistance they provided during the blast experiments. Special thanks to Matt Smith of National Oilwell Varco for donating the FRP tubes, and Peter Glaude and Serge Doyan for their machining and fabrication work. Also, the assistance provided by Masoud Mehrraoui and Kevin Zmetra during construction and axial capacity testing is very much appreciated. The authors are very appreciative of Fyfe for the donation of the fire-protection system for the fire experiments and Brian Flaherty for the donation of the flame-retardant coating used during blast testing.

References

- AASHTO. (2011). *Guide specifications for LRFD seismic bridge design*, 2nd Ed., Washington, DC.
- AASHTO. (2012a). *LRFD bridge design specifications*, 6th Ed., Washington, DC.
- AASHTO. (2012b). *LRFD guide specifications for design of concrete-filled FRP tubes for flexural and axial members*, Washington, DC.
- Alipour, A., Shafei, B., and Shinouzuka, M. (2010). "Failure estimation of highway bridges under combined effects of scouring and earthquake." *Proc., 5th Int. Conf. on Bridge Maintenance, Safety, and Management*, IABMAS, Philadelphia.
- Alipour, A., Shafei, B., and Shinouzuka, M. (2011). "Performance evaluation of deteriorating highway bridges located in high seismic areas." *J. Bridge Eng.*, **10.1061/(ASCE)BE.1943-5592.0000197**, 597–611.
- Alipour, A., Shafei, B., and Shinouzuka, M. (2013). "Reliability-based calibration of load and resistance factors for design of RC bridges under multiple extreme events: Scour and earthquake." *J. Bridge Eng.*, **10.1061/(ASCE)BE.1943-5592.0000369**, 362–371.
- Aquino, W., and Hawkins, N. M. (2007). "Seismic retrofitting of corroded reinforced concrete columns using carbon composites." *ACI Struct. J.*, **104**(3), 348–356.
- Basoz, N., and Kiremidjian, A. S. (1998). "Evaluation of bridge damage data from the Loma Prieta and Northridge, California earthquakes." *Rep. No. MCEER-98-0004*, Univ. at Buffalo, Buffalo, NY.
- Berger, J. O., Heffernan, P. J., and Wight, R. G. (2013). "Blast testing of CFRP and SRP strengthened RC columns." *Design against blast: Load definition and structural response*, 189.
- Bisby, L. A., Kodur, V. K. R., and Green, M. F. (2005). "Fire endurance of fiber-reinforced polymer-confined concrete columns." *ACI Struct. J.*, **102**(6), 883–891.
- Bruneau, M., El-Bahey, S., Fujikura, S., and Keller, D. (2011). "Structural fuses and concrete-filled steel shapes for seismic- and multi-hazard resistant design." *Bull. New Zealand Soc. Earthquake Eng.*, **44**(1), 44–52.
- Caltrans (California Department of Transportation). (2006). *Seismic design criteria version 1.4*, Sacramento, CA.
- Chang, Y. F., Chen, Y. H., Sheu, M. S., and Yao, G. C. (2006). "Residual stress-strain relationship for concrete after exposure to high temperatures." *Cement Concr. Res.*, **36**(10), 1999–2005.
- Choe, D. E., Gardoni, P., Rosowsky, D., and Haukaas, T. (2008). "Probabilistic capacity models and seismic fragility estimates for RC columns subjected to corrosion." *Reliabil. Eng. Syst. Safety*, **93**(3), 383–393.
- Choe, D. E., Gardoni, P., Rosowsky, D., and Haukaas, T. (2009). "Seismic fragility estimates for reinforced concrete bridges subject to corrosion." *Struct. Safety*, **31**(4), 275–283.
- Correal, J. F., Saiidi, M., and Sanders, D. H. (2004). "Seismic performance of RC bridge columns reinforced with two interlocking spirals." *Rep. No. CCEER-04-06*, Univ. of Nevada, Reno, NV.
- Cruz Noguez, C. A., and Saiidi, M. (2012). "Shake-table studies of a four-span bridge model with advanced materials." *J. Struct. Eng.*, **10.1061/(ASCE)ST.1943-541X.0000457**, 183–192.
- DHS (Department of Homeland Security). (2009). *Bomb threat stand-off chart*, Washington, DC.
- Echevarria, A., Zaghi, A. E., Christenson, R., and Chiarito, V. (2014a). "The seismic, blast and fire resilience of concrete-filled FRP tube (CFFT) bridge columns." *Proc., IABMAS 2014*, IABMAS, Shanghai, China.
- Echevarria, A., Zaghi, A. E., Chiarito, V., Christenson, R., and Woodson, S. (2014b). "Experimental comparison of the performance and residual capacity of CFFT and RC bridge columns subjected to blasts." *J. Bridge Eng.*, in press.
- Fam, A. (2000). "Concrete-filled fiber-reinforced polymer tubes for axial and flexural structural members." Ph.D. dissertation, Univ. of Manitoba, Winnipeg, MB.
- Fam, A., Cole, B., and Mandal, S. (2007). "Composite tubes as an alternative to steel spirals for concrete members in bending and shear." *Constr. Build. Mater.*, **21**(2), 347–355.
- Fam, A., Flisak, B., and Rizkalla, S. (2003). "Experimental and analytical modeling of concrete-filled fiber-reinforced polymer tubes subjected to combined bending and axial loads." *ACI Struct. J.*, **100**(4), 499–509.
- Fam, A., and Rizkalla, S. (2002). "Flexural behavior of concrete-filled fiber-reinforced polymer circular tubes." *J. Compos. Constr.*, **10.1061/(ASCE)1090-0268(2002)6:2(123)**, 123–132.
- FEMA. (2012). "Multi-hazard loss estimation methodology." *Hazus—MH 2.1*, Washington, DC.
- FHWA. (2011). "Framework for improving resilience of bridge design." *Publication No. FHWA-IF-11-016*, Washington, DC.

- FHWA (Federal Highway Administration). (2006). "Blast design and analysis for highway structures." (<http://www.fhwa.dot.gov/publications/focus/06aug/02.cfm>) (Mar. 2, 2013).
- Franchin, P., and Pinto, P. E. (2007). "Transitability of mainshock-damaged bridges." *Proc., 1st US-Italy Seismic Bridge Workshop*, IUSS Press, Pavia, Italy.
- Franchin, P., and Pinto, P. E. (2009). "Allowing traffic over mainshock-damaged bridges." *J. Earthquake Eng.*, 13(5), 585–599.
- Fujikura, S., and Bruneau, M. (2008). "Blast resistance of seismically designed bridge piers." *Proc., 14th World Conf. on Earthquake Engineering*, International Association for Earthquake Engineering, Dallas, TX.
- Fujikura, S., and Bruneau, M. (2011). "Experimental investigation of seismically resistant bridge piers under blast loading." *J. Bridge Eng.*, 10.1061/(ASCE)BE.1943-5592.0000124, 63–71.
- Fujikura, S., and Bruneau, M. (2012). "Dynamic analysis of multihazard resistant bridge piers having concrete-filled steel tube under blast loading." *J. Bridge Eng.*, 10.1061/(ASCE)BE.1943-5592.0000270, 249–258.
- Fujikura, S., Bruneau, M., and Lopez-Garcia, D. (2007). "Experimental investigation of blast performance of seismically resistant concrete-filled steel tube bridge piers." *Rep. No. MCEER-07-005*, Univ. at Buffalo, Buffalo, NY.
- Fujikura, S., Bruneau, M., and Lopez-Garcia, D. (2008). "Experimental investigation of multihazard resistant bridge piers having concrete-filled steel tube under blast loading." *J. Bridge Eng.*, 10.1061/(ASCE)1084-0702(2008)13:6(586), 586–594.
- Fyfe. (2013). "Tyfo® CFP System." (<http://www.fyfeco.com/Products/Fire-Resistant-Systems.aspx>) (Jan. 15, 2013).
- Gefu, J., Li, G., Li, X., Pang, S., and Jones, R. (2008). "Experimental study of FRP tube encased concrete cylinders exposed to fire." *Compos. Struct.*, 85(2), 149–154.
- Ghosh, J., and Padgett, J. E. (2010). "Aging considerations in the development of time-dependent seismic fragility curves." *J. Struct. Eng.*, 10.1061/(ASCE)ST.1943-541X.0000260, 1497–1511.
- Ghosh, J., Padgett, J. E., and Sanchez-Silva, M. (2015). "Seismic damage accumulation of highway bridges in earthquake prone regions." *Earthquake Spectra*, 31(1), 115–135.
- IABMAS (International Association for Bridge Maintenance And Safety). (2012). "Bridge maintenance, safety, management, resilience and sustainability." *Proc., 6th Int. IABMAS Conf.*, Stress, Italy.
- Imbsen Software Systems. (2007). *XTract*, TRC, Sacramento, CA.
- Itani, A., Gaspersic, P., and Saiidi, M. (1997). "Response modification factors for seismic design of circular reinforced concrete bridge columns." *ACI Struct. J.*, 94(1), 23–30.
- Kavianipour, F., and Saiedi, M. (2012). "Shake table testing of a quarter-scale 4-span bridge with composite piers." *Proc., 6th IABMAS*, Politecnico Di Milano, Stresa, Italy, 1966–1973.
- Keller, D., Fujikura, S., Fouche, P., and Bruneau, M. (2009). "Multi-hazard (blast, seismic, tsunamis, collision) resistant bridge piers." *80th Shock and Vibration Symp. (SAVIAC)*, Shock and Vibration Exchange, Arvonia, VA.
- Kodur, V. K. R., Bisby, L. A., and Green, M. F. (2007). "Preliminary guidance for the design of FRP-strengthened concrete members exposed to fire." *J. Fire Protect. Eng.*, 17(1), 5–26.
- Kowalsky, M. J., Priestly, M. J. N., and MacRae, G. A. (1995). "Displacement-based design of RC bridge columns in seismic regions." *Earthquake Eng. Struct. Dyn.*, 24(12), 1623–1643.
- Kumar, R., and Gardoni, P. (2012). "Modeling structural degradation of RC bridge columns subjected to earthquakes and their fragility estimates." *J. Struct. Eng.*, 10.1061/(ASCE)ST.1943-541X.0000450, 42–51.
- Kyodo News. (2011). "Survivors on cut-off isle were ready for disaster." (<http://www.japantimes.co.jp/news/2011/03/19/news/survivors-on-cut-off-isle-were-ready-for-disaster/#>) (May 1, 2014).
- Lam, L., and Teng, J. G. (2003). "Design-oriented stress-strain model for FRP-confined concrete." *Constr. Build. Mater.*, 17(6–7), 471–489.
- Lee, G. C., Mohan, S. B., Huang, C., and Fard, B. N. (2013). "A study of U.S. bridge failures." *Technical Rep. No. MCEER-13-0008*, Univ. at Buffalo, Buffalo, NY.
- Li, J., Gong, J., and Wang, L. (2009). "Seismic behavior of corrosion-damaged reinforced concrete columns strengthened using combined carbon fiber-reinforced polymer and steel jacket." *Constr. Build. Mater.*, 23(7), 2653–2663.
- Liang, L., and Lee, G. C. (2013). "Towards establishing practical multi-hazard bridge design limit states." *Earthquake Eng. Eng. Vibr.*, 12(3), 333–340.
- Mirmiran, A., and Shahawy, M. (1995). "A novel FRP-concrete composite construction for the infrastructure." *Proc., ASCE Structures Congress XIII*, ASCE, Reston, VA, 1663–1666.
- Mirmiran, A., and Shahawy, M. (1996). "A new concrete-filled hollow FRP composite column." *Compos. Eng.*, 27B(3–4), 263–268.
- Mirmiran, A., and Shahawy, M. (1997). "Behavior of concrete columns confined by fiber composites." *J. Struct. Eng.*, 10.1061/(ASCE)0733-9445(1997)123:5(583), 583–590.
- Mirmiran, A., Shahawy, M., Khouri, C. E., and Naguib, W. (2000). "Large beam-column tests on concrete-filled composite tubes." *ACI Struct. J.*, 97(2), 268–276.
- Mirmiran, A., Shahawy, M., and Samaan, M. (1999). "Strength and ductility of hybrid FRP-concrete beam-columns." *J. Struct. Eng.*, 10.1061/(ASCE)0733-9445(1999)125:10(1085), 1085–1093.
- Mohamed, H. M., and Masmoudi, R. (2010). "Axial load capacity of concrete-filled FRP tube columns: Experimental versus theoretical predictions." *J. Compos. Constr.*, 10.1061/(ASCE)CC.1943-5614.0000066, 231–243.
- Mortensen, J., and Saiidi, M. (2002). "A performance-based design method for confinement in circular columns." *Rep. No. CCEER 02-07*, Univ. of Nevada, Reno, NV.
- Muszynski, L. C., and Purcell, M. R. (2003). "Composite reinforcement to strengthen existing concrete structures against air blast." *J. Compos. Constr.*, 10.1061/(ASCE)1090-0268(2003)7:2(93), 93–97.
- National Academy of Sciences. (2014). "Resilience at the national academies." (<http://www.nationalacademies.org/topics/resilience/index.html>) (Dec. 29, 2014).
- NOV Fiberglass Systems. (2009). "Red thread II piping systems." (<http://www.corrosionfluid.com/assets/pdfsmith-fibercast-red-thread-2-ii-fiberglass-pipe-piping-brochure.pdf>) (Feb. 16, 2012).
- PEER (Pacific Earthquake Engineering Research Center). (2012). "OpenSees v2.4.2." (<http://opensees.berkeley.edu>) (Jul. 20, 2012).
- Prasad, G. G., and Banerjee, S. (2013). "The impact of flood-induced scour on seismic fragility characteristics of bridges." *J. Earthquake Eng.*, 17(6) 803–828.
- Priestley, M. J. N. (2000). "Performance based seismic design." *Proc., 12th WCEE*, International Association for Earthquake Engineering, Dallas, TX.
- Priestley, M. J. N., Seible, F., and Calvi, G. M. (1996). *Seismic design and retrofit of bridges*, Wiley, New York.
- Roknaddin, K., Ghosh, J., Duenas-Osorio, L., and Padgett, J. E. (2013). "Bridge retrofit prioritisation for ageing transportation networks subjected to seismic hazards." *Struct. Infrastruct. Eng. Maintenance Manage. Life Cycle Des. Perform.*, 9(10), 1050–1066.
- Rong, H., and Li, B. (2008). "Deformation-controlled design of reinforced concrete flexural members subjected to blast loadings." *J. Struct. Eng.*, 10.1061/(ASCE)0733-9445(2008)134:10(1598), 1598–1610.
- Saadatmanesh, H., Ehsani, M. R., and Jin, L. (1996). "Seismic strengthening of circular bridge pier models with fiber composites." *ACI Struct. J.*, 93(6), 639–647.
- Shao, Y. (2003). "Behavior of FRP-concrete beam-columns under cyclic loading." Ph.D. thesis, North Carolina State Univ., Raleigh, NC.
- Shao, Y., and Mirmiran, A. (2004). "Nonlinear cyclic response of laminated glass FRP tubes filled with concrete." *Compos. Struct.*, 65(1), 91–101.
- Shao, Y., and Mirmiran, A. (2005). "Experimental investigation of cyclic behavior of concrete-filled fiber reinforced polymer tubes." *J. Compos. Constr.*, 10.1061/(ASCE)1090-0268(2005)9:3(263), 263–273.
- Sheikh, A. A., and Yau, G. (2002). "Seismic behavior of concrete columns confined with steel and fiber-reinforced polymers." *ACI Struct. J.*, 99(1), 72–80.

- Simon, J., Bracci, J. M., and Gardoni, P. (2010). "Seismic response and fragility of deteriorated reinforced concrete bridges." *J. Struct. Eng.*, **10.1061/(ASCE)ST.1943-541X.0000220**, 1273–1281.
- Spacey, J. (2011). "Japan Talk." (<http://www.japan-talk.com/jt/new/21-scary-statistics-about-the-2011-japan-earthquake>) (Apr. 30, 2014).
- Wang, H., and Saiidi, M. (2005). "A study of RC columns with shape memory alloy and engineered cementitious composites." *Rep. No. CCEER-05- 1*, Univ. of Nevada, Reno, NV.
- Williamson, E. B., et al. (2010). "Blast-resistant highway bridges: Design and detailing guidelines." *NCHRP Rep. 465*, Transportation Research Board, Washington, DC.
- Williamson, E. B., and Winget, D. G. (2005). "Risk management and design of critical bridges for terrorist attacks." *J. Bridge Eng.*, **10.1061/(ASCE)1084-0702(2005)10:1(96)**, 96–106.
- Winget, D. G., Williamson, E. B., Marchand, K. A., and Gannon, J. C. (2005). "Recommendations for blast design and retrofit of typical highway bridges." *Transportation Research Record*, Transportation Research Board, Washington, DC, 1–8.
- Wright, W., Lattimer, B., Woodworth, M., Nahid, M., and Sotelino, E. (2013). "NCHRP project 12-85: Highway bridge fire hazard assessment draft final report." Transportation Research Board, Washington, DC.
- Zaghi, A. E., Saiidi, M., and Mirmiran, A. (2012). "Shake table response and analysis of a concrete-filled FRP tube bridge column." *Compos. Struct.*, **94**(5), 1564–1574.
- Zhu, Z., Ahmad, I., and Mirmiran, A. (2006). "Seismic performance of concrete-filled FRP tube columns for bridge substructure." *J. Bridge Eng.*, **10.1061/(ASCE)1084-0702(2006)11:3(359)**, 359–370.
- Zhu, Z., Mirmiran, A., and Shahawy, M. (2004). "Stay-in-place FRP forms for precast modular bridge pier system." *J. Compos. Constr.*, **8**(6), 560–568.
- Zohrevand, P., and Mirmiran, A. (2013). "Seismic response of ultra-high performance concrete-filled FRP tube columns." *J. Earthquake Eng.*, **17**(1), 155–170.